

## Supporting Information

### Thermal treatment effects on PMN-0.4PT/Fe multiferroic heterostructures

*Deepak Dagur<sup>a</sup>, Alice Margherita Finardi<sup>ab</sup>, Vincent Polewczyk<sup>a</sup>, Aleksandr Yu. Petrov<sup>a</sup>, Simone Dolabella<sup>a</sup>, Federico Motti<sup>a</sup>, Hemanita Sharma<sup>ac</sup>, Edvard Dobovicnik<sup>d</sup>, Andrea Giugni<sup>ab</sup>, Giorgio Rossi<sup>ab</sup>, Claudia Fasolato<sup>e</sup>, Piero Torelli<sup>a</sup>, and Giovanni Vinai<sup>a\*</sup>*

<sup>a</sup>CNR - Istituto Officina dei Materiali (IOM), S.S. 14 km 163.5, I-34149, Trieste, Italy

<sup>b</sup>Department of Physics, University of Milan, Milan, Via Festa del Perdono 7, 20122, Italy

<sup>c</sup>Department of Physics, University of Trieste, Trieste, Via Alfonso Valerio 2, 34127, Italy

<sup>d</sup>Department of Engineering and Architecture, University of Trieste, Trieste, Via Alfonso Valerio 2, 34127, Italy

<sup>e</sup>Istituto dei Sistemi Complessi (ISC)-CNR, Rome, Piazzale Aldo Moro 5, 00185, Italy

\*E-mail: [vinai@iom.cnr.it](mailto:vinai@iom.cnr.it)

## PMN<sub>0.4</sub>PT polarization switching

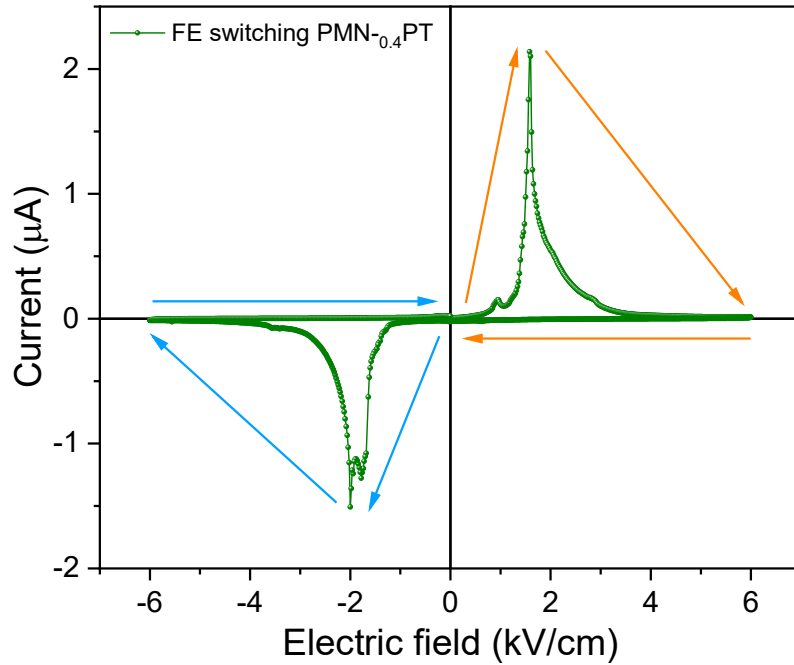


**Figure S1:** I(E) curve of PMN<sub>0.4</sub>PT (001) heterostructure, showing ferroelectric transitions around  $\pm 2$  kV cm<sup>-1</sup>.

To confirm the ferroelectric behavior of PMN<sub>0.4</sub>PT substrate, I(E) curves were recorded by applying an electric field up to  $\pm 6$  kV cm<sup>-1</sup> through the thickness of the substrate, sweeping the field along the [001] crystallographic direction from -6 to +6 kV cm<sup>-1</sup> and then back to zero (**Figure S1**). Stable FE transitions were recorded around  $\pm 2$  kV cm<sup>-1</sup>, consistently with what previously reported by our group on similar substrates.<sup>1,2</sup>

## XRD characterization

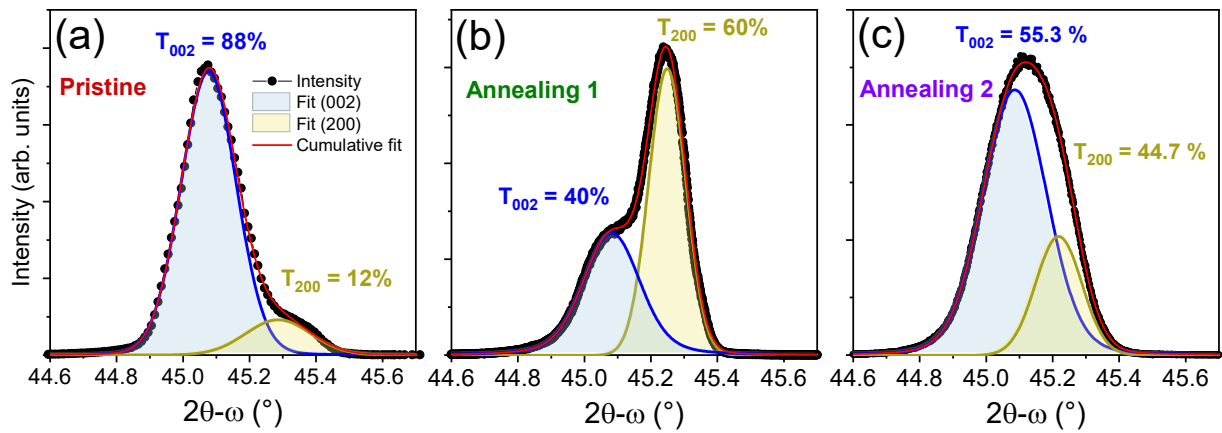


**Figure S2:** (a-c) XRD  $2\theta$ - $\omega$  scans for pristine and after the two thermal treatments of PMN<sub>0.4</sub>PT/Fe heterostructure, with relative fittings of the (002) and (200)/(020) contributions for the three cases.

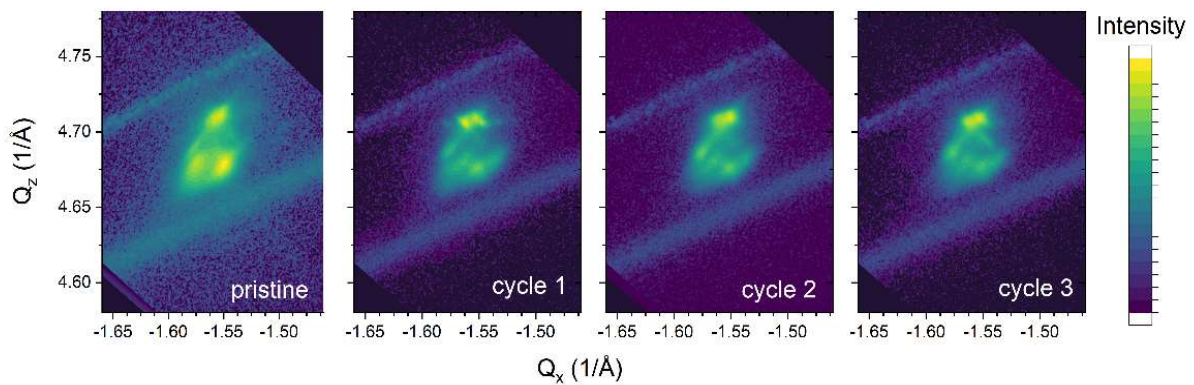


**Figure S3:** 2D RSMs of a PMN<sub>0.4</sub>PT crystal in pristine and after different thermal cycles in “annealing 1” condition.

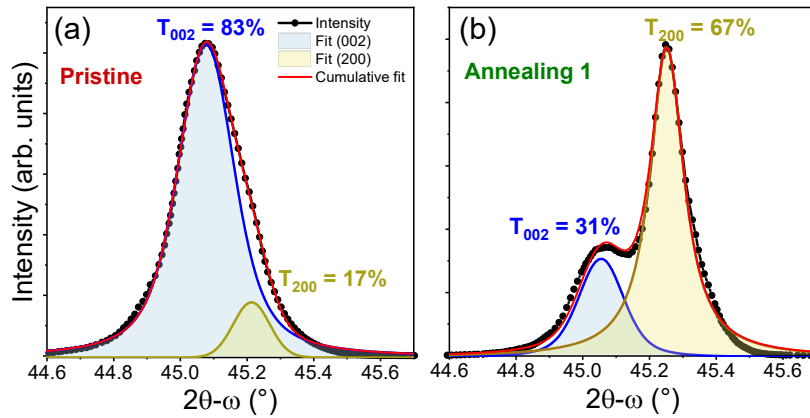


**Figure S4:** XRD  $2\theta$ - $\omega$  scans of pristine unannealed and after the first thermal treatment of PMN-<sub>0.4</sub>PT/Fe heterostructure used for Raman characterizations.

XRD symmetric  $2\theta$ - $\omega$  scans were taken on PMN-<sub>0.4</sub>PT/Fe heterostructure, as shown in **(Figure S2 and S4)**, on which the same phase analysis was repeated. A similar evolution of the ratios between the in-plane and out-of-plane domains was observed as a function of the thermal annealing treatments, proving both a good reproducibility of the process in terms of modification of the structural properties of PMN-<sub>0.4</sub>PT substrate and a negligible role played by the interfacial layer.

## micro-Raman characterization

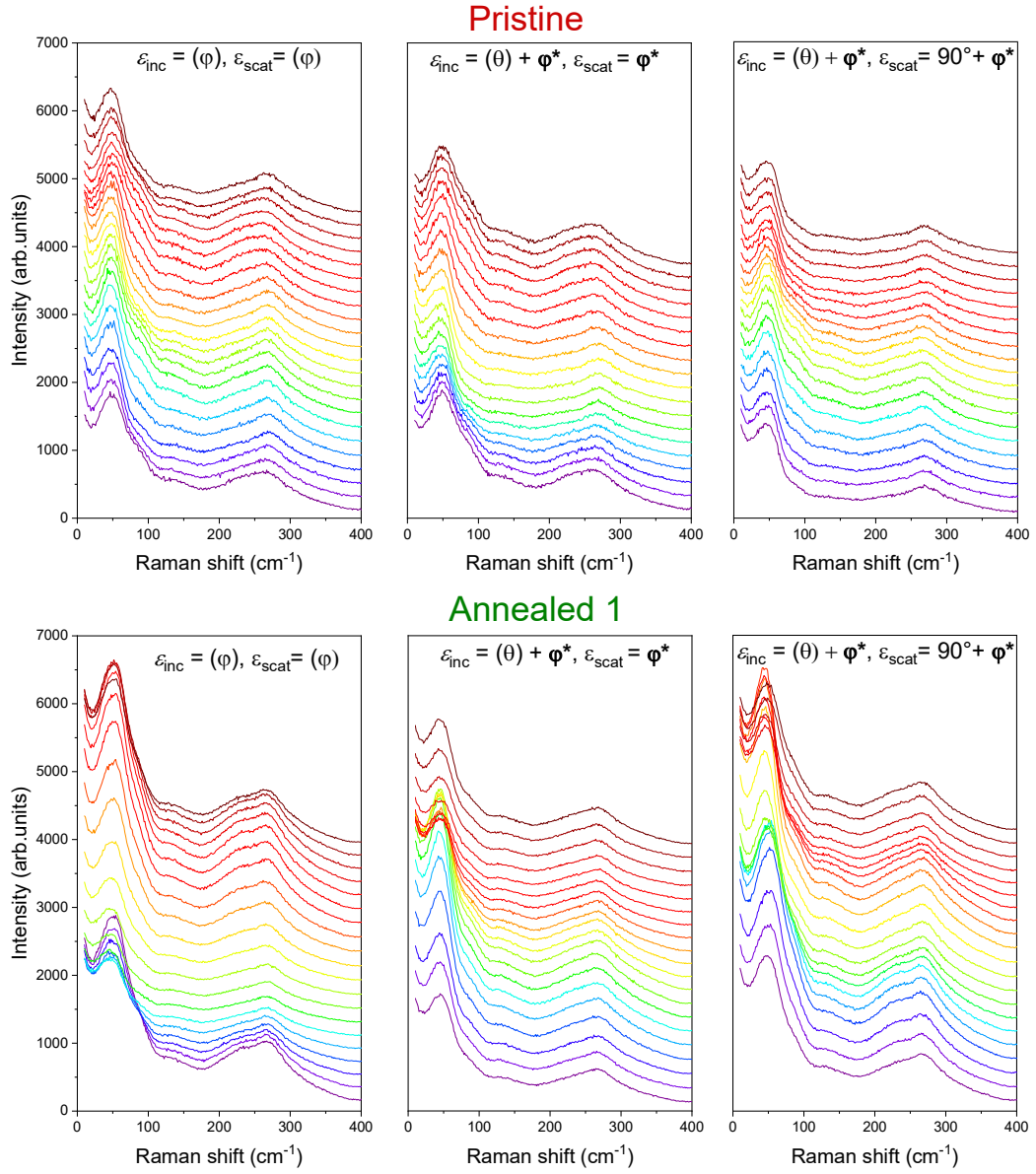


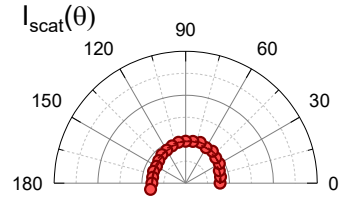
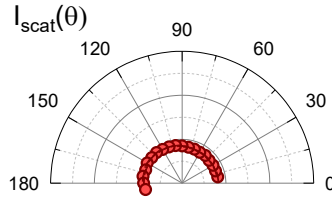
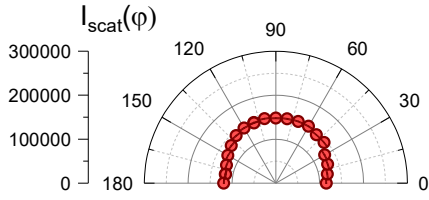
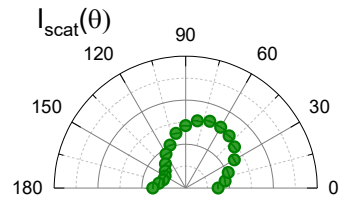
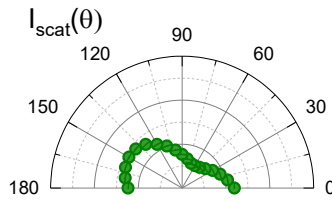
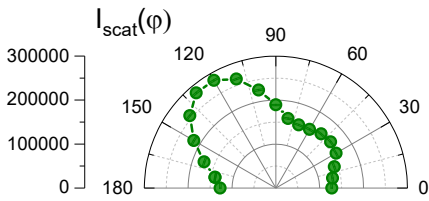
**Figure S5:** Polarization dependent Raman spectra of PMN<sub>0.4</sub>PT/Fe heterostructure in the three polarization configurations for pristine unannealed and annealed 1 case. Polarization notation as in Figure 4 of the main text.

**A2**

$\varepsilon_{\text{inc}} = (\varphi), \varepsilon_{\text{scat}} = (\varphi)$

$\varepsilon_{\text{inc}} = (\theta) + \varphi^*, \varepsilon_{\text{scat}} = \varphi^*$

$\varepsilon_{\text{inc}} = (\theta) + \varphi^*, \varepsilon_{\text{scat}} = 90^\circ + \varphi^*$

**Pristine****Annealing 1**

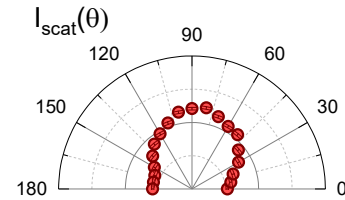
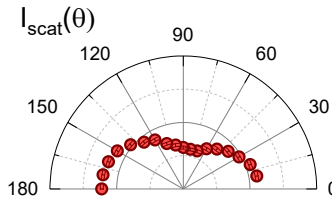
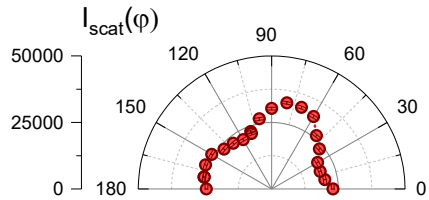
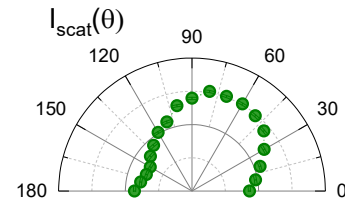
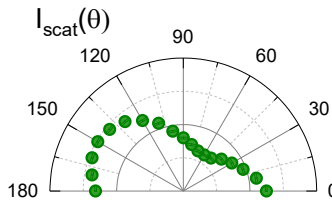
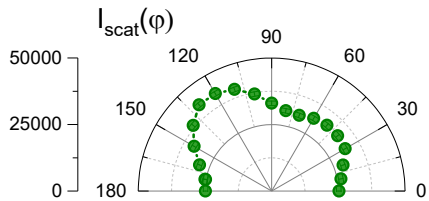
**Figure S6:** Polar plots of the **A2** Raman mode intensity acquired on PMN-<sub>0.4</sub>PT/Fe (001) heterostructures (pristine and annealed 1) in the three polarization configurations indicated above.

**A5**

$\varepsilon_{\text{inc}} = (\varphi), \varepsilon_{\text{scat}} = (\varphi)$

$\varepsilon_{\text{inc}} = (\theta) + \varphi^*, \varepsilon_{\text{scat}} = \varphi^*$

$\varepsilon_{\text{inc}} = (\theta) + \varphi^*, \varepsilon_{\text{scat}} = 90^\circ + \varphi^*$

**Pristine****Annealing 1**

**Figure S7:** Polar plots of the **A5** Raman mode intensity acquired on PMN-<sub>0.4</sub>PT/Fe (001) heterostructures (pristine and annealed 1) in the three polarization configurations indicated above.

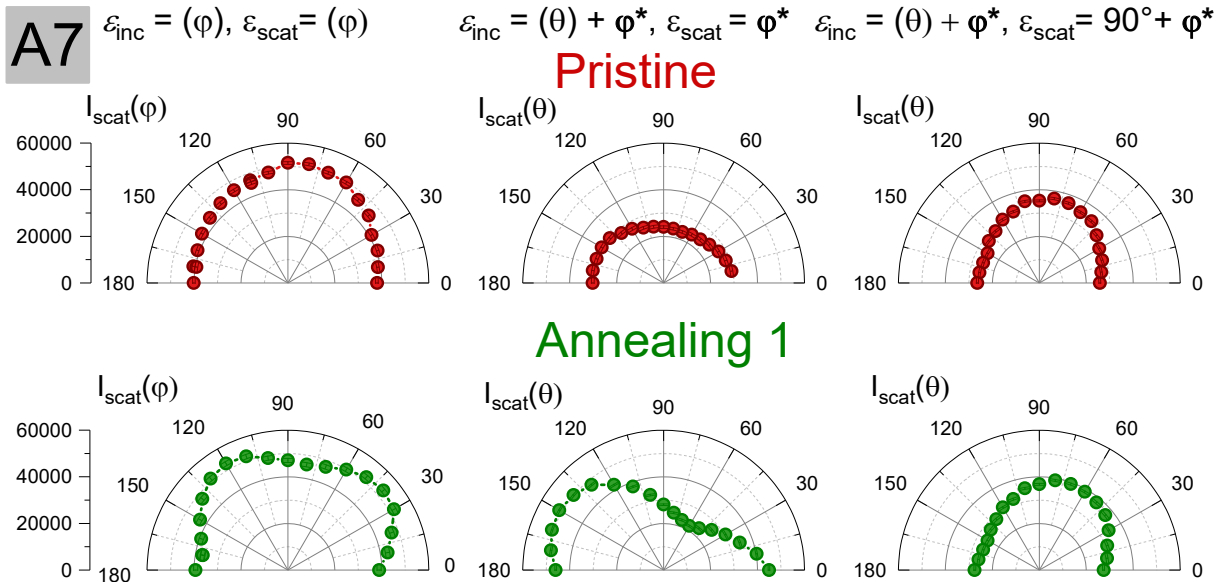


**Figure S8:** Polar plots of the A7 Raman mode intensity acquired on PMN-<sub>0.4</sub>PT/Fe (001) heterostructures (pristine and annealed 1) in the three polarization configurations indicated above.

## MOKE characterization

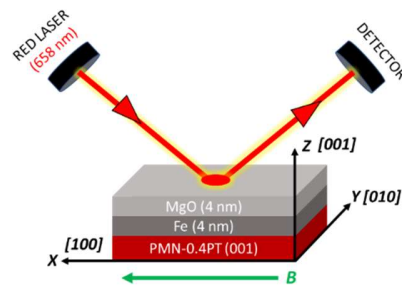


**Figure S9:** Schematic representation of the PMN<sub>0.4</sub>PT/Fe heterostructure and experimental setup of longitudinal MOKE. A He-Ne laser of 658 nm wavelength was used.

**Figure S9** shows the sample stack of the PMN<sub>0.4</sub>PT/Fe heterostructure and the schematics of the setup used for longitudinal MOKE measurements. The magnetic hysteresis loops and polar plots were measured by applying an in-plane magnetic field with respect to the surface of the sample. The angle convention used for the polar plots assigns 0° for  $B$  along [010] PMN-PT direction and 90° along [100]. An example of polar plots and angle dependent MOKE measurement is shown in **Figure S10** for PMN<sub>0.4</sub>PT/Fe sample after annealing 1 procedure.

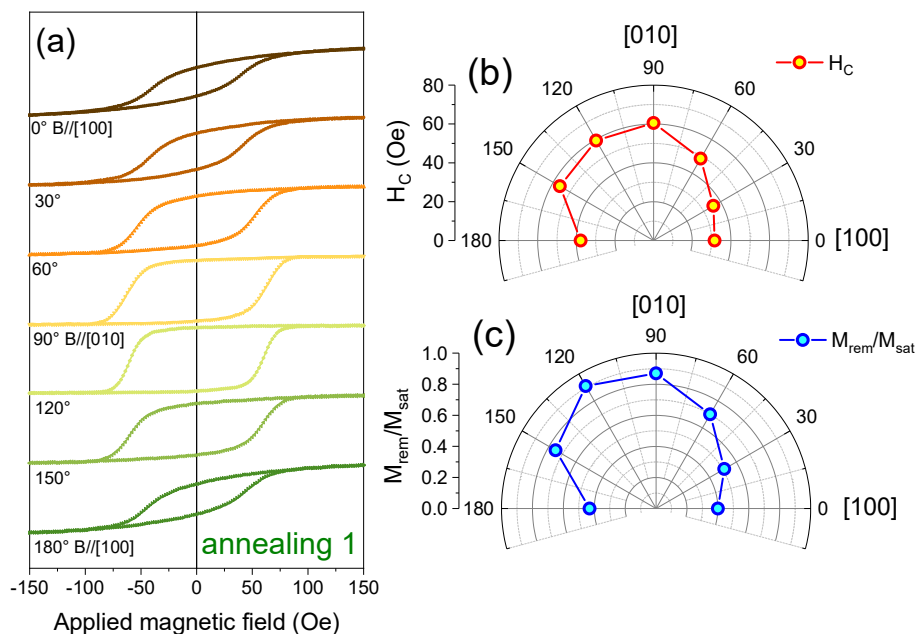


**Figure S10:** (a) angle dependent hysteresis loops of PMN<sub>0.4</sub>PT/Fe heterostructure after annealing 1, with the corresponding polar plots of (b) coercive field and (c) magnetic remanence.



## References

- (1) Vinai, G.; Motti, F.; Bonanni, V.; Petrov, A. Y.; Benedetti, S.; Rinaldi, C.; Stella, M.; Cassese, D.; Prato, S.; Cantoni, M.; Rossi, G.; Panaccione, G.; Torelli, P. Reversible Modification of Ferromagnetism through Electrically Controlled Morphology *Adv. Electron. Mater.* **2019**, *5* (7), 1900150.
- (2) Motti, F.; Vinai, G.; Bonanni, V.; Polewczyk, V.; Mantegazza, P.; Forrest, T.; Maccherozzi, F.; Benedetti, S.; Rinaldi, C.; Cantoni, M.; Cassese, D.; Prato, S.; Dhesi, S. S.; Rossi, G.; Panaccione, G.; Torelli, P. Interplay between Morphology and Magnetoelectric Coupling in Fe/PMN-PT Multiferroic Heterostructures Studied by Microscopy Techniques *Phys. Rev. Mater.* **2020**, *4* (11), 114418.